IOPscience iopscience.iop.org

Home Search Collections Journals About Contact us My IOPscience

The electronic structure of orthorhombic Al_2Ru

This article has been downloaded from IOPscience. Please scroll down to see the full text article.

1997 J. Phys.: Condens. Matter 9 7999

(http://iopscience.iop.org/0953-8984/9/38/007)

View the table of contents for this issue, or go to the journal homepage for more

Download details:
IP Address: 171.66.16.209
The article was downloaded on 14/05/2010 at 10:34

Please note that terms and conditions apply.

J. Phys.: Condens. Matter **9** (1997) 7999–8010. Printed in the UK PII: S0953-8984(97)81682-7

The electronic structure of orthorhombic Al_2Ru

Vincent Fournée†, Esther Belin-Ferré†¶, Guy Trambly de Laissardière‡, Anne Sadoc§, Pavel Volkov‖ and S Joseph Poon‖

† LCPMR, URA CNRS 176, and GDR CINQ, 11 rue Pierre et Marie Curie, 75231 Paris Cédex 05, France

‡ LEPES-CNRS and GDR CINQ, 25 Avenue des Martyrs, BP 166X, 38042 Grenoble, and LLB, Bâtiment 563, CEA-Saclay, 91191 Gif-sur-Yvette Cédex, France

§ LURE, Bâtiment 209D, 91405 Orsay Cédex, and LPMS and GDR CINQ, Université de Cergy-Pontoise, Bâtiment des Sciences de la Matière, Neuville sur Oise, F-95031 Cergy-Pontoise Cédex, France

‖ Department of Physics, University of Virginia, Charlottesville, VA 22901, USA

Received 7 February 1997, in final form 6 May 1997

Abstract. We present the results of an investigation, both theoretical and experimental, of partially occupied and unoccupied electronic distributions in orthorhombic Al_2Ru. The occupied Al states near E_F are p–d hybridized in interaction with Ru 4d states, whereas they are almost purely s-like in character beyond 6 eV from E_F. The Ru 4d states are found close to E_F; their interaction with the Al states produces an important depletion of the Al 3s–d and Al 3p distributions. As a result, the Al edges are somewhat pushed back from E_F. Thus a wide range of energy with almost no states is present in the occupied band side. E_F lies close to the bottom of the unoccupied band where both unoccupied Al states and unoccupied Ru states are present. These results are compared to previous data for icosahedral quasicrystalline $Al_{70.5}Pd_{21}Re_{8.5}$.

1. Introduction

For many years now, investigation of the electronic structure of quasicrystalline intermetallics has given impetus to the study of related crystalline alloys. The existence of a marked pseudo-gap at the Fermi level (E_F) appears to be important for quasicrystals, as has been observed experimentally (Traverse *et al* 1988, Matsuo *et al* 1989, Matsubara *et al* 1991, Mori *et al* 1991, Belin *et al* 1992a, b, Hippert *et al* 1992, Stadnik and Stroink 1993) and predicted theoretically on the basis of densities-of-states (DOS) calculations performed for crystalline approximants (Fujiwara 1990, Fujiwara and Yokokawa 1991, Phillips and Rabe 1991, Hafner and Krajci 1993, Krajci and Hafner 1992). Many physical and electronic properties have been related to the existence of this pseudo-gap (see for example Poon (1992) and references therein, Berger *et al* (1993), Berger (1994) and references therein, and Krajci *et al* (1995)), in particular the high resistivity, especially at low temperature, displayed by most of the stable icosahedral quasicrystals of high structural quality (Belin-Ferré and Dubois 1996).

Several Al-based crystalline alloys also exhibit a marked non-metallic behaviour (Pierce *et al* 1993, Volkov and Poon 1995, Poon 1996) which is *a priori* unexpected, since Al,

¶ Author to whom any correspondence should be addressed: Esther Belin-Ferré, Laboratoire de Chimie Physique—Matière et Rayonnement, URA CNRS 176, and GDR CINQ, 11 rue Pierre et Marie Curie, 75231 Paris Cédex 05, France; telephone: +33 1 44 27 66 20; fax: +33 1 44 27 62 26; e-mail: belin@ccr.jussieu.fr.

0953-8984/97/387999+12$19.50 © 1997 IOP Publishing Ltd

which is the major component, is a very good metal. Thus, it is of interest to investigate the electronic structure of such intermetallics to enable a meaningful comparison with quasicrystals to be made.

The purpose of this work is to analyse by experimental as well as theoretical means the electronic structure of orthorhombic Al_2Ru. This binary alloy displays semiconductor-like behaviour (Basov *et al* 1994), it belongs to the same phase diagram as quasicrystalline $Al_{65}Cu_{20}Ru_{15}$, and its Al and transition metal contents are comparable to those of the quasicrystal. Note that, for $Al_{65}Cu_{20}Ru_{15}$, resistivities at low temperature as high as 30 000 $\mu\Omega$ cm have been reported (Biggs *et al* 1991), and the presence of a rather wide and deep pseudo-gap at E_F has been seen experimentally using photoemission (XPS) (Stadnik *et al* 1994, Nakamura and Mizutani 1994) as well as soft-x-ray spectroscopy (SXS) techniques (Belin-Ferré *et al* 1996).

The paper is organized as follows. In sections 2 and 3, we briefly describe the experimental techniques and procedures which we have carried out in making the measurements. Section 4 gives information about the methodology of our calculations. Section 5 describes and compares the experimental and theoretical results. All of these results are discussed in section 6 and summarized in section 7.

2. Experimental techniques

The experimental techniques and spectral analysis have already been described elsewhere (see for example Belin-Ferré *et al* 1996). Let us recall that the soft x-ray emission and absorption spectroscopy (SXES and SXAS respectively) techniques are both of spectral character and atomic site selective. The SXS processes are governed by dipole selection rules. The energy distributions are proportional to $N_{(\varepsilon)}$, which denotes the partially occupied or unoccupied DOS of the solid analysed (the OB and the UB respectively), and to $L(n, l)$ which is the width of the inner level involved in the x-ray transition. The matrix elements of the SXS transition probabilities are either constant or vary slowly with energy, so, usually, they do not need to be accounted for. These techniques display no absolute DOS values, but it is possible to compare given spectral distribution curves for various materials to investigate possible modifications of the electronic structure.

The spectral distribution curves are obtained each on its own x-ray transition energy scale. Adjustment to an absolute energy scale may be achieved by setting E_F into each x-ray transition energy scale. For such a purpose, the binding energies of the inner levels involved in the SXS transitions are measured by means of XPS experiments. Thus it is possible to trace the spectral distributions on the binding energy scale.

3. Experimental procedure

The orthorhombic Al_2Ru sample which we used was investigated by means of x-ray measurements and low-temperature conductivity by Pierce *et al* (1993). We probed various x-ray transitions to describe occupied as well as unoccupied bands (table 1). Let us mention that for Ru, the L$\beta_{2,15}$ spectrum accounts mainly for the occupied 4d-state distribution, since x-ray transition probabilities favour p–d transitions over p–s ones; in addition, note that the s-state contribution is already significantly faint in the OB of pure Ru (Papaconstantopoulos 1986a, b).

Let us recall briefly that the SXES spectra were scanned with vacuum spectrometers fitted with bent SiO_2 crystals ($10\bar{1}0$ or $11\bar{2}0$ planes) or a grating, whose final energy

Table 1. The x-ray transition analysed, the states investigated, the energy range studied, the experimental technique, and the width of the inner level involved in the x-ray transition (the widths of the inner levels are from Krause and Oliver (1979)).

X-ray transition	State investigated	Energy range (eV)	Technique	Width of the inner level (eV)
Al Kβ: OB $\rightarrow$ 1s	Al 3p	1550–1565	SXES	~ 0.4
Al $L_{2,3}$: OB $\rightarrow$ $2p_{3/2}$	Al 3s–d	55–75	SXES	< 0.1
Ru L$\beta_{2,15}$: OB $\rightarrow$ $2p_{3/2}$	Ru 3s–d	2827–2847	SXES	~ 2.0
Al K: 1s $\rightarrow$ UB	Al p	1555–1585	SXAS	~ 0.4
Ru L_{III}: $2p_{3/2}$ $\rightarrow$ UB	Ru s–d	2830–2850	SXAS	~ 2.0

resolutions were about 0.35 eV for Al 3s, d, 0.45 eV for Al 3p, and about 2 eV for Ru 4d states. The SXAS experiments were performed at the synchrotron facility of the Laboratoire pour l'Utilisation du Rayonnement Electromagnétique (LURE, Orsay, France). Measurements involve the yield technique at the Super ACO storage ring (experimental station SA 32) applied by means of a two-crystal monochromator equipped with SiO_2 $10\bar{1}0$ slabs. The final energy resolutions were 0.45 eV for Al K and 2.5 eV for Ru L_{III} spectra. SXS spectra of fcc Al and hcp Ru were also recorded for comparison and calibration purposes. All of the spectral curves were normalized between their maximum intensity and ranges where their variation of intensity is negligible.

The Al $2p_{3/2}$ and Ru 3p binding energies were measured with an XPS spectrometer fitted with a Mg cathode. For Ru, since we did not scan the 4d-level binding energy, we assumed a constant chemical shift in the alloy with respect to pure metal. The Al 1s binding energy was deduced from the energies of the Al $2p_{3/2}$ level and the Al Kα ($2p_{3/2} \rightarrow 1s$) x-ray emission line (Traverse *et al* 1988). Finally, we could place E_F on the various x-ray transition energy scales within ± 0.2 eV for Al and ± 0.3 eV for Ru.

4. Densities-of-states calculations

Al_2Ru is face-centred orthorhombic ($Fddd$ or C54), and each unit cell contains six atoms: four Al atoms and two Ru atoms. The lattice parameters are $a = 0.8015$ nm, $b = 0.4715$ nm, and $c = 0.8780$ nm (Pearson 1967). A calculation of the electronic structure has already been reported by Nguyen Manh *et al* (1992), who pointed out the hybridization between Ru d and Al p states and the formation of a gap at E_F. In our paper, we focus on the partial DOSs. To achieve a meaningful comparison with the experimental data, we have smoothed out the partially occupied and unoccupied DOSs first by using a Lorentzian-like distribution to account for the intrinsic SXS broadening due to the inner level (table 1) and second by using a Gaussian distribution to account for the instrumental function (0.3 eV). We obtained thus calculated SXS spectra which we denote as CS in the following.

5. Results

We will not show here the total DOS curve that has been given by Nguyen Manh *et al* (1992), but rather the partial DOSs, which we display in figure 1 (from bottom to top: theoretical Al s, Al p, Al d, and Ru s and Ru d partial DOS curves). The Ru d states are dominant, since their maximum intensity is 6.21 states eV^{-1} per unit cell as against 0.2 for

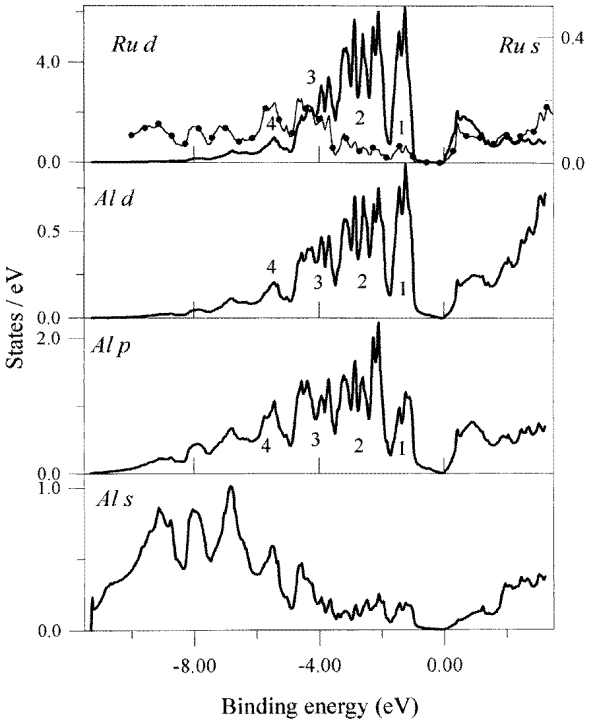

Figure 1. Calculated partial DOSs. From bottom to top: Al s, Al p, Al d, and Ru s (dotted line) and Ru d (full line) partial distributions.

Ru s, 2.23 for Al p, 1.01 for Al s, and 0.89 for Al d. The Al s and Ru s states are mostly located below $E_F - 4$ eV, towards high binding energies. The curves for the Al p, Al d, and Ru d states exhibit roughly the same shape, namely four sets of peaks. Note that the intensities of all of the partial DOSs beyond about 1 eV from E_F are dramatically low.

The occupied Al 3p, both occupied Al 3s and 3d, and unoccupied Al p CS, as well as experimental curves, are shown in figures 2 and 3 respectively. The corresponding theoretical partial DOSs are also given for the sake of comparison. Let us begin with the Al 3p-like occupied distributions (figure 2). The partial DOS curve (lowest panel) exhibits various sets of peaks over about 10 eV marked A, B_1 and B_2, C_1 and C_2, D, and F, and a wide hollow denoted as E. The maximum intensity is that of peak B_1. The CS (middle panel) is a broad smooth peak showing several faint fluctuations of intensity labelled a, b_2, c_1 and c_2, d, and e that correspond to A, B_2, C_1 and C_2, D, and E. The maximum b is in coincidence not with peak B_1 but with a secondary peak of the DOS curve shown by a double arrow in the figure. Within about 1 eV of E_F the intensity of the CS is very low but not equal to zero. The shape of the experimental Al 3p distribution curve (uppermost panel) compares well with that of the CS since the various features of both curves are in the same energy ranges. However, several inversions of intensities are observed between experiment and theory: the maximum β_2 coincides with the secondary peak B_2 whereas the faint concave shoulder β_1 corresponds to the maximum B_1. The experimental intensity at E_F is comparable to that of the CS. This low intensity near E_F will be discussed in the next section. The large peak P of the theoretical p-like unoccupied DOS is seen as a marked bump p on the CS. The edge of the DOS curve is straight and close to E_F; some intensity

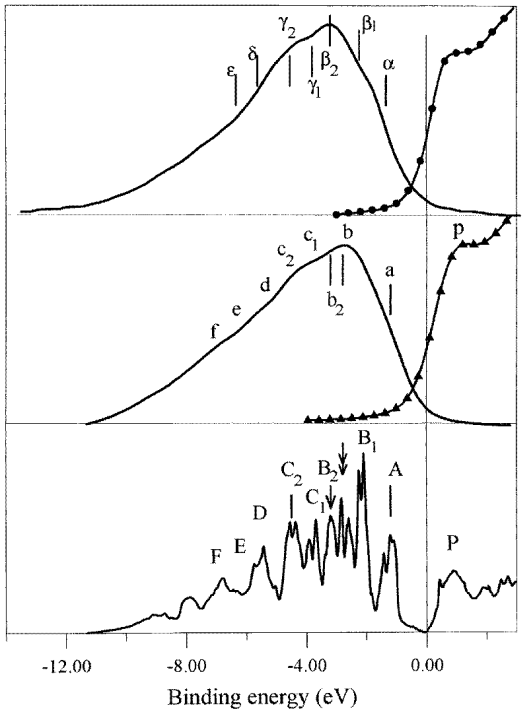

Figure 2. Al 3p distributions. Lowest panel: the theoretical Al p DOS. Middle panel: the calculated Al Kβ spectrum (see the text). Uppermost panel: the occupied Al 3p experimental distribution (full line) and the Al p unoccupied experimental distribution (dotted line). For an explanation of the labels, see the text.

is observed at E_F in the CS. The unoccupied Al p-state experimental and CS curves are in fair agreement.

The three panels of figure 3 display s and d Al distribution curves. In the lowest panel we show the Al s DOS and its corresponding CS curves. The middle panel shows the same curves for Al d-like character. In the uppermost panel, the experimental Al 3s, d spectrum is plotted together with a curve obtained from the sum of the s DOS with two-fifths of the d DOS that, according to Goodings and Harris (1969), allows us to account for the differences between p $\rightarrow$ s and p $\rightarrow$ d transition probabilities. The peaks labelled A_1, A_3, B, C, and D_1 of the Al s DOS curve coincide with the peaks (or sets of peaks) marked I, II, III, IV, and V of the Al d DOS curve. The corresponding CS curves exhibit features coinciding in energy with those of the DOS curves. The edge of the d-like CS arises from the broadening of peak I. The maximum of the s-like CS corresponds to peak D_1. That of the d-like CS curve corresponds to feature a_3; it is roughly at the energy of the centroid of the set of peaks denoted as II. Whereas the s DOS and d DOS intensities are almost zero at E_F, some faint intensity is observed for the corresponding CS curves. We will come back to this point in the next section. Within the experimental precision, the features of the experimental curve coincide with the structures of both the s and d CS curves. However, discrepancies can be noticed for the intensities: the intensities of features α_1 and α_3 are the reverse of those of the structures a_1 and a_3; on the other hand, the intensity of feature δ_1 is noticeably higher than that of feature δ_2, whereas the intensities of structures

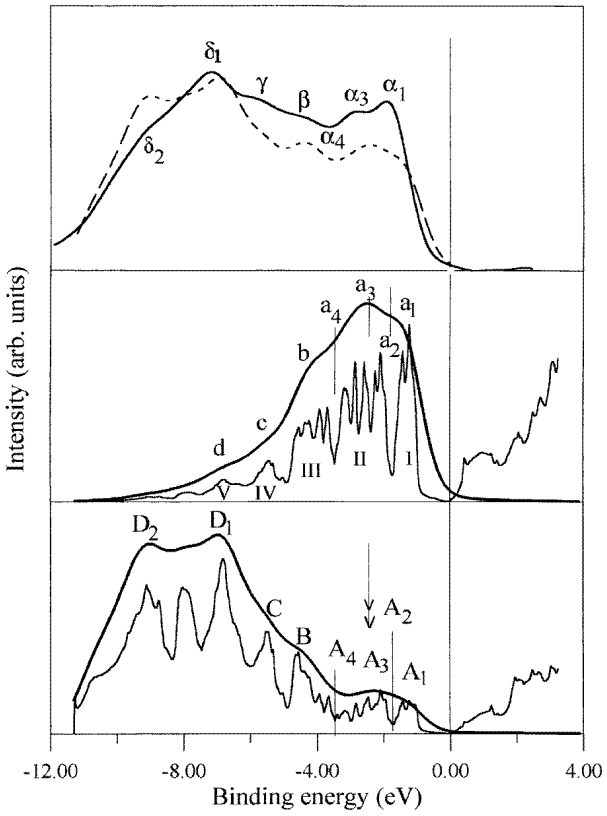

Figure 3. Al 3s–d distributions. Lowest panel: the theoretical (thin line) and broadened (thick line) Al s DOS (see the text). Middle panel: the theoretical (thin line) and broadened (thick line) Al d DOS (see the text). Uppermost panel: the occupied Al 3s–d experimental distribution (full line). The dotted curve has been obtained from the sum of the broadened s DOS with two-fifths of the d DOS to account for differences between p → s and p → d transition probabilities (see the text).

D_1 and D_2 are almost equal. No broadening of the partially unoccupied s and d DOSs has been carried out since no experimental data are available for us to compare them with.

Figure 4 displays the Ru L$\beta_{2,15}$ curves for pure hcp metal and for the alloy. Let us recall that these curves mainly reflect the Ru 4d-state distribution. The same shape as for the pure metal is preserved in the alloy, consistently with the fact that d states, being of rather localized character, are less sensitive than p or s states to any modification of the atomic environment. The full width at half-maximum intensity is reduced by 1 ± 0.1 eV in the alloy, and the maximum is shifted by 0.6 ± 0.1 eV towards high binding energies. We have plotted on the same figure, figure 4, the spectra obtained for unoccupied d and s states in pure hcp Ru and Ru in Al_2Ru. The curve for pure Ru exhibits a sharp 'white line' A, followed by two structures labelled B and C. The curve of the alloy retains a peak in the same energy range as peak A but it is much less intense and somewhat broadened; in addition, there are no features in the energy ranges of B and C.

Finally, figure 5 shows a sketch of the occupied and unoccupied distributions in Al_2Ru. For comparison, the Al 3p experimental curve for pure fcc Al is also plotted on the same figure, also normalized to its own maximum intensity.

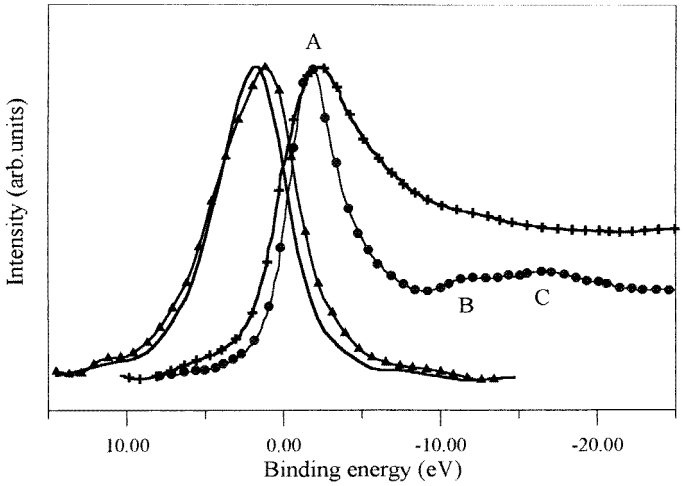

Figure 4. Ru 4d occupied and Ru d–s unoccupied distributions in pure hcp metal (triangles and dots respectively) and in Al_2Ru (full line and crosses respectively).

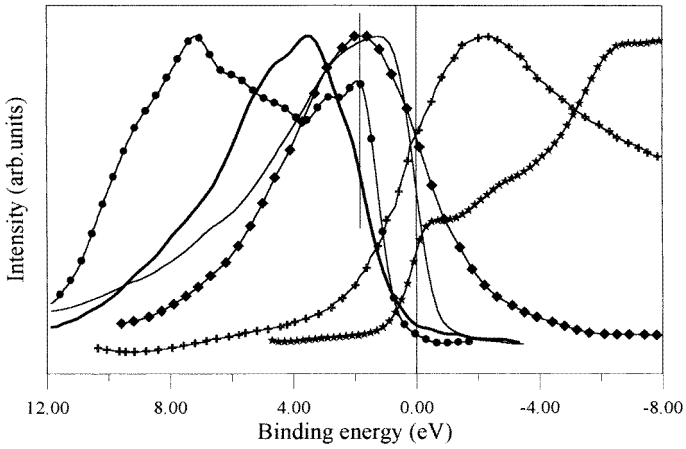

Figure 5. Occupied (left-hand side) and unoccupied (right-hand side) electronic distributions of Al_2Ru as obtained experimentally. Full line: Al 3p states; dotted line: Al 3s–d states; line with squares: Ru 4d states; starred line: Al p states; line with crosses: Ru d–s states. The thin full line corresponds to Al 3p states in pure fcc Al.

6. Discussion

To begin the discussion, let us recall results obtained using the same experimental procedure for pure metals. For pure fcc Al (see for example Belin-Ferré *et al* 1996), the inflexion point of the steep Al 3p edge is exactly at E_F and its intensity is half the maximum intensity of the Al 3p sub-band (figure 5). The Al 3s–d curve exhibits a prominent peak near E_F which is characteristic of a free-electron-like metal. The Al 3p-state and Al 3s–d-state distribution curves totally overlap, revealing strong s–p hybridization over the whole occupied band with some s–p–d hybridization at and near E_F. In pure hcp Ru, the 4d-state distribution curve

(figure 4) consists of a large almost symmetric peak. Peak A of the unoccupied d–s curve is due to transitions from p $\rightarrow$ d-like states. Structure B results from the transition from p $\rightarrow$ s–d hybridized states. The same should hold true for feature C (Papaconstantopoulos 1986a, b).

For Al_2Ru the shapes and energy extent of the various sub-bands differ from those for the pure metals, revealing thus genuine hybridizations. The peaks of the Al p and Al d DOS curves of the calculation of Nguyen Manh *et al* (1992) coincide within the range that covers 6 eV from E_F (figure 1). Accordingly, the Al states within this energy range are p–d hybridized. Then, below $E_F - 6$ eV they are almost purely s-like in character. Unoccupied states are also hybridized but they are of dominant p-like character within the first 2 eV from E_F. Our experimental results confirm the results of these calculations. They show significant overlap between Al 3p and 3s, d curves within the $E_F - 6$ eV region, and also with Ru 4d states in this energy range. This is seen in figure 5, where we have traced a vertical line to stress that the d-like states from Al and from Ru are completely mixed, thus involving strong energetic overlap of the corresponding orbitals. Terakura (1977) discussed interaction between localized and extended states. He pointed out that the extended states split into two distinct bonding and non-bonding parts located on each side of the energy position of the maximum of the d states, and exhibit a relative minimum intensity at the energy of the maximum of the d states. In addition, the d-like states are shifted from the energy position that they had without interaction. In Al_2Ru, as compared to pure fcc Al, due to this type of interaction in the vicinity of E_F, the Al sub-bands are pushed away from E_F. This is clearly shown in figure 5 where the Al 3p distribution in pure fcc Al is plotted; this emphasizes the strong depletion of Al 3p states over 1 eV below E_F in the alloy. Thus, around E_F, the intensities of the occupied part of the Al electronic distributions is significantly weak. This is in agreement with NMR measurements made by Hill *et al* (1995) on the same Al_2Ru sample that have indicated a very low residual DOS at E_F and an important chemical shift of the Al NMR signal.

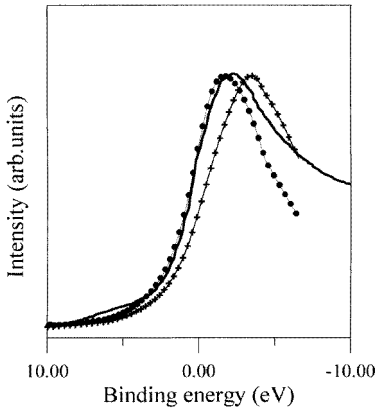

Figure 6. Broadened unoccupied Ru s (crosses) and d (dots) DOSs and the experimental Ru d–s curve (full line) of Al_2Ru.

In section 5, we mentioned that the Ru d states are also slightly repelled from E_F. Their distribution is narrower than in the hcp metal, consistently with the fact that there are fewer Ru neighbours in the alloy than in the metal. So, the intensity at E_F is decreased in the alloy with respect to pure hcp Ru. We have also pointed out that the Ru unoccupied states are less peaked in Al_2Ru than in the pure metal. To go further, we compare in figure 6

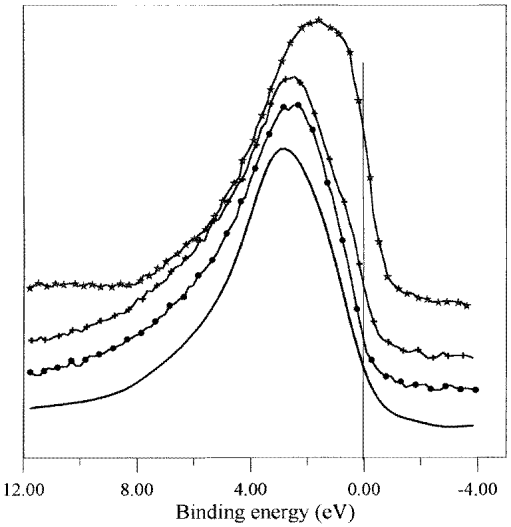

Figure 7. From bottom to top: experimental Al 3p distributions in Al_4Re (full line), $Al_{13}Fe_4$ (dotted line), Al_5Co_2 (crossed line), and Al_6Mn (starred line).

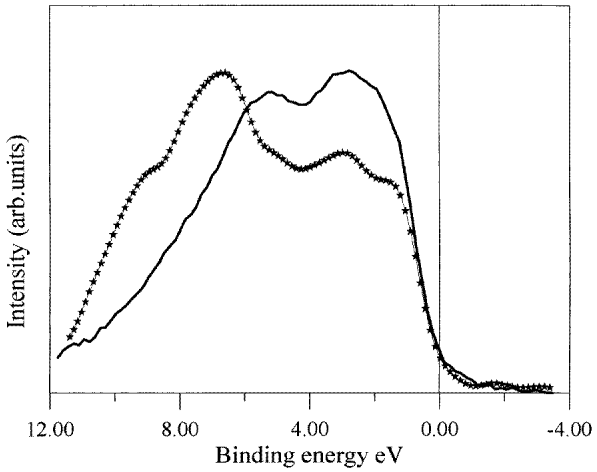

Figure 8. Al 3p (full line) and Al 3s–d (starred line) experimental electronic distributions in $Al_{70.5}Pd_{21}Re_{8.5}$.

the experimental curve and the CS curves obtained from the theoretical partial Ru s and d unoccupied DOSs. This confirms that over about 1 eV beyond E_F, the Ru states are of d-like character, although it is less marked than for the pure metal; then they are mixed with states that are s-like in character.

Finally, our results show that both occupied and unoccupied bands in Al_2Ru are lined by states of localized-like character, namely d or mixed d–p states.

Let us now discuss the faint intensity contribution of the OB Al CS curves at E_F or in its vicinity. Let us recall that these curves result from the broadening of the partial DOS to account for both the inner level involved in the x-ray transitions and the experimental

resolution. It is worth noticing the very fair agreement with the experimental results: this confirms that the small intensity which is observed from experiments is mainly an artefact due to the broadening of the DOS, which is inherent to the SXS techniques as well as because of the instrumental functions. Thus, for Al_2Ru, both experiments and calculations show that the actual Al DOSs in the vicinity of E_F are almost vanishingly small. Accordingly, this emphasizes the very strong interaction between Al and Ru states. The excellent agreement between experiment and calculation confirms that this near gap is present mostly in the occupied band of Al_2Ru: indeed, the distance from E_F of the Al 3p distribution edge taken at half the maximum intensity of the sub-band (denoted as δ) is 1.1 ± 0.1 eV in the alloy, whereas it is, by definition, 0 in pure fcc Al. This clearly demonstrates that the electronic properties of the alloy should dramatically depart from those of a free-electron-like system. Note that in the Al p unoccupied counterpart, the 'gap' is almost non-existent.

Using the same experimental methodology as for Al_2Ru, we have investigated the electronic structure of quasicrystalline icosahedral $Al_{65}Cu_{20}Ru_{15}$ and $Al_{70.5}Pd_{21}Re_{8.5}$ (Belin *et al* 1995, Belin-Ferré *et al* 1996). To summarize, we have shown the formation of a pseudo-gap in their Al state distribution: for example, in $Al_{65}Cu_{20}Ru_{15}$, the distance d is 0.60 ± 0.05 eV; the Al densities of states at E_F, although rather low as compared to those for pure fcc Al, are not as faint as for Al_2Ru. For this quasicrystal, a charge transfer from Al and Cu atoms to the Ru ones was suggested (Belin-Ferré *et al* 1996), and an EXAFS investigation indicated chemical ordering, and Al–Cu and Al–Ru distances of 0.251 nm and 0.261 nm respectively were measured (Sadoc *et al* 1995): the Ru–Al bond was found to be 5.7% shorter than the sum of the Al and Ru atomic radii, which is 0.277 nm. In Al_2Ru, the strong interaction between Al and Ru states is confirmed by the small interatomic distances (0.257 and 0.264 nm)—noticeably shorter than the sum of the Al and Ru atomic radii. Therefore, the Al–Ru bonding appears to be somewhat covalent, in line with the wide 'near gap' found in the Al DOS. This also reflects a strong chemical ordering of Ru and Al. Note that the 0.261 nm Ru–Al distance measured for $Al_{65}Cu_{20}Ru_{15}$ corresponds to the average value of the two Ru–Al distances in Al_2Ru.

Other binary Al–transition metal alloys do not display such wide pseudo-gaps. For example, in monoclinic $Al_{13}Fe_4$ (Traverse *et al* 1996) and in hexagonal Al_5Co_2 (Pêcheur *et al* 1995, Belin-Ferré *et al* 1997b), which are approximants of quasicrystalline structures, δ is 0.65 ± 0.05 eV and 0.55 ± 0.05 eV respectively, and it is 0.80 ± 0.05 eV in monoclinic Al_4Re (Belin-Ferré *et al* 1997a) as is mapped out in figure 9, and 0.20 ± 0.05 in Al_6Mn (Belin and Traverse 1991). In all of these alloys, the intensities at E_F are 15%, 22%, 20%, and 48% in $Al_{13}Fe_4$, Al_5Co_2, Al_4Re, and Al_6Mn respectively, to be compared to 50% for fcc Al (see section 5). In the framework of the normalization of the Al 3p partial sub-band to its maximum, we have mentioned that the intensity at E_F is 0.5; then if we ascribe the value 1 free electron to pure fcc Al, it would correspond to ascribing 0.3, 0.44, 0.40, and 0.96 free electrons to $Al_{13}Fe_4$, Al_5Co_2, Al_4Re, and Al_6Mn respectively. Low values indicate that the free-electron model is no longer valid for explaining the electronic properties of the corresponding alloy; the lower the value, the more the alloy departs from the free-electron model. As an example, for quasicrystalline Al–Li–Cu alloy, such an adjustment has given 0.3 free electrons, which is in good agreement with results from specific heat measurements (Hippert *et al* 1992).

$Al_{13}Fe_4$ exhibits metallic behaviour along the *b*-axis and non-metallic behaviour along the pseudo-quasiperiodic axis, whereas Al_4Re behaves rather like a semiconductor. We found generally large δ and low intensity at E_F for alloys displaying high resistivities at low temperatures, whereas δ is smaller and the Al 3p intensity at E_F is higher in materials that are not as resistive (Belin-Ferré and Dubois 1996). Thus, the presence of a large

deep pseudo-gap in the Al 3p electronic distribution of Al_2Ru that is in addition framed by localized-like states may account for the doped-semiconductor-like behaviour of this alloy as reported by Basov *et al* (1994).

Let us compare to the case of icosahedral quasicrystalline $Al_{70.5}Pd_{21}Re_{8.5}$. The distance δ and the Al 3p intensity at E_F have been found to be 1.2 ± 0.1 eV and 7% respectively (Belin and Traverse 1991) (figure 10). The Pd–Al and Re–Al distances measured by EXAFS are all 0.260 nm (Sadoc *et al* 1995)—namely 7.1% shorter than the sum of the atomic radii, thus emphasizing the somewhat covalent bonding. For Al_2Ru, d is similar but the value of the intensity at E_F is only about 5%. Consequently, this would correspond to 0.14 free electrons for $Al_{70.5}Pd_{21}Re_{8.5}$ and less than $\simeq$0.1 free electrons for Al_2Ru. We have deduced that the faint intensity observed experimentally for Al_2Ru in ranges where there are almost no states according to theoretical calculations is an experimental artefact. Our results have shown that there are actually very few states in the pseudo-gap present in quasicrystalline icosahedral $Al_{70.5}Pd_{21}Re_{8.5}$ (Belin *et al* 1995). According to our data for Al_2Ru, we suggest that there is almost a true 'gap' in icosahedral quasicrystalline $Al_{70.5}Pd_{21}Re_{8.5}$. Such a view is in accordance with the extremely high resistivity at low temperature displayed by this alloy. Let us recall that it can be of the same order of magnitude as that found for genuine semiconductors, like Si.

7. Conclusion

We have presented in this paper the results of a joint theoretical and experimental investigation of partially occupied and unoccupied electronic distributions in orthorhombic Al_2Ru. We have shown that, in the occupied band, the Al states near E_F are p–d hybridized, whereas they are almost purely s-like in character beyond 6 eV from E_F. Ru 4d states are found close to E_F. They overlap the Al d-like state. The strong interaction between the Ru 4d states and the Al states produces an important depletion of the Al sub-bands, the result of which is to somewhat push the corresponding edges far from E_F. This gives rise to the formation of a wide energy '*near gap*' in agreement with the semiconducting properties of this alloy. This '*gap*' is found to mainly exist in the occupied band side, whereas both Al p and Ru d and d–s unoccupied states are present just at and above E_F. The current results agree with previous investigations of electronic distributions of various intermetallics using the same methodology, and, in particular, they are analogous to our results for icosahedral quasicrystalline $Al_{70.5}Pd_{21}Re_{8.5}$. We suggest that the pseudo-gap that we observed in this latter alloy might instead be *almost a real gap* with a finite faint density of states within it. This is in line with its very high resistivity at low temperature, whose order of magnitude is similar to that of genuine semiconductors.

Acknowledgments

We are indebted to D Nguyen Manh and D Mayou for invaluable discussions. We thank A M Flank and P Lagarde for assistance with making the measurements at LURE. This work was supported in part by the Austrian Ministry of Research, East–West Cooperation programme, under the title 'Soft X-ray Emission Spectroscopy of Metallic Systems'. We gratefully acknowledge Professor H Kirchmayr and Doctor H Müller for hospitality at the Technical University in Vienna.

References

Basov D N, Pierce F S, Volkov P, Poon S J and Timusk T 1994 *Phys. Rev. Lett.* **73** 1865

Belin E, Dankházi Z, Sadoc A, Flank A M, Poon J S, Müller H and Kirchmayr H 1995 *Proc. 5th Int. Conf. on Quasicrystals* ed C Janot and R Mosseri (Singapore: World Scientific) p 435

Belin E, Dankházi Z, Sadoc A, Klein T, Calvayrac Y and Dubois J M 1992a *J. Phys.: Condens. Matter* **4** 4459

Belin E, Kojnok J, Sadoc A, Traverse A, Harmelin M and Dubois J M 1992b *J. Phys.: Condens. Matter* **4** 1057

Belin E and Traverse A 1991 *J. Phys.: Condens. Matter* **3** 2157

Belin-Ferré E, Dankházi Z, Sadoc A, Berger C, Müller H and Kirchmayr H 1996 *J. Phys. Condens. Matter* **8** 3513

Belin-Ferré E, Dankházi Z, Sadoc A and Poon J S 1997a unpublished

Belin-Ferré E and Dubois J M 1996 *J. Phys.: Condens. Matter* **8** L717

Belin-Ferré E, Trambly de Laissardière G, Pêcheur P, Sadoc A and Dubois J M 1997b submitted

Berger C 1994 *Lectures on Quasicrystals* (Les Ulis: Editions de Physique) p 463

Berger C, Belin E and Mayou D 1993 *Ann. Chim.* **18** 485

Biggs B D, Poon S J and Munirathnam N R 1991 *Phys. Rev. Lett.* **65** 2700

Fujiwara T 1990 *J. Non-Cryst. Solids* **117+118** 844

Fujiwara T and Yokokawa T 1991 *Phys. Rev. Lett.* **66** 333

Goodings D A and Harris R 1969 *J. Phys. C: Solid State Phys.* **2** 1808

Hafner J and Krajci M 1993 *Phys. Rev.* B **47** 11 795

Hill E A, Volkov P, Poon S J and Wu Y 1995 *Phys. Rev.* B **51** 4865

Hippert F, Kandel L, Calvayrac Y and Dubost B 1992 *Phys. Rev. Lett.* **69** 2086

Krajci M and Hafner J 1992 *Phys. Rev.* B **46** 10 669

Krajci M, Windisch M, Hafner J and Kresse G 1995 *Phys. Rev.* B **51** 17 355

Krause M O and Oliver J H 1979 *J. Phys. Chem. Ref. Data* **8** 329

Matsubara H, Ogawa S, Kinoshita T, Kishi K, Takeuchi S, Kimura K and Suga S 1991 *Japan. J. Appl. Phys.* **30** L389

Matsuo S, Nakano H, Ishimasa T and Fukano Y 1989 *J. Phys.: Condens. Matter* **3** 6893

Mori M, Matsuo S, Ishimasa T, Matsuura T, Kamiya K, Inokuchi H and Matsukawa T 1991 *J. Phys.: Condens. Matter* **3** 767

Nakamura Y and Mizutani U 1994 *Mater. Sci. Eng.* A **181+182** 790

Nguyen Manh D, Trambly de Laissardière G, Julien J P, Mayou D and Cyrot-Lackmann F 1992 *Solid State Commun.* **82** 329

Papaconstantopoulos D A 1986a *Handbook of the Band Structures of Elemental Solids* (New York: Plenum) p 208 (for Al)

——1986b *Handbook of the Band Structures of Elemental Solids* (New York: Plenum) p 149 (for Ru)

Pêcheur P, Belin E, Toussaint G, Trambly de Laissardière G, Mayou D, Dankházi Z, Müller H and Kirchmayr H 1995 *Proc. 5th Int. Conf. on Quasicrystals* ed C Janot and R Mosseri (Singapore: World Scientific)

Pearson W P 1967 *Handbook of Lattice Spacings and Structures of Metals* (Oxford: Pergamon)

Phillips J C and Rabe K M 1991 *Phys. Rev. Lett.* **66** 923

Pierce F S, Poon S J and Biggs B D 1993 *Phys. Rev. Lett.* **70** 3919

Poon S J 1992 *Adv. Phys.* **41** 303

——1996 *Proc. Conf. on New Horizons in Quasicrystals: Research and Applications*

Sadoc A, Poon S J and Boudard M 1995 *Proc. 5th Int. Conf. on Quasicrystals* ed C Janot and R Mosseri (Singapore: World Scientific) p 156

Stadnik Z M and Stroink G 1993 *Phys. Rev.* B **47** 100

Stadnik Z M, Zhang G W, Tsai A P and Inoue A 1994 *J. Phys.: Condens. Matter* **6** 1097

Terakura K 1977 *J. Phys. F: Met. Phys.* **9** 1773

Traverse A, Belin-Ferré E, Dankházi Z, Mendoza-Zélis L, Laborde O and Portier R 1996 *J. Phys.: Condens. Matter* **8** 3843–57

Traverse A, Dumoulin L, Belin E and Sénémaud C 1988 *Quasicrystalline Materials (ILL/CODEST Workshop)* ed C Janot and J M Dubois (Singapore: World Scientific) p 399

Volkov P and Poon S J 1995 *Phys. Rev.* B **52** 1